INTERNATIONAL JOURNAL FOR NUMERICAL METHODS IN FLUIDS
Int. J. Numer. Meth. Fluids 2003; **43**:199–213 (DOI: 10.1002/fld.608)

The partition-of-unity method for linear diffusion and convection problems: accuracy, stabilization and multiscale interpretation

E. A. Munts*,†, S. J. Hulshoff and R. de Borst

Delft University of Technology, Faculty of Aerospace Engineering, P.O. Box 5058, 2629 HS Delft, The Netherlands

SUMMARY

We investigate the effectiveness of the partition-of-unity method (PUM) for convection–diffusion problems. We show that for the linear diffusion equation, an exponential enrichment function based on an approximation of the analytic solution leads to improved accuracy compared to the standard finite-element method. It is illustrated that this approach can be more efficient than using polynomial enrichment to increase the order of the scheme. We argue that the PUM enrichment, can be interpreted as a subgrid-scale model in a multiscale framework, and that the choice of enrichment function has consequences for the stabilization properties of the method. The exponential enrichment is shown to function as a near optimal subgrid-scale model for linear convection. Copyright © 2003 John Wiley & Sons, Ltd.

KEY WORDS: finite-element method; partition-of-unity method; convection; diffusion; stabilization

1. INTRODUCTION

The partition-of-unity method [1–3], also known as 'generalized' or 'extended' finite-element method, has emerged as a powerful technique for incorporating special functions into the finite-element method. These special functions, also called 'enrichment functions', can be chosen based on approximate analytic solutions in order to provide a better approximation than can be obtained from standard polynomial shape functions. This feature was clearly demonstrated by Strouboulis *et al.* [4], who considered the Laplacian in domains with several elliptical voids. In this case, superior accuracy was obtained by incorporating harmonic basis functions corresponding to the problem of the elliptical void in an infinite medium. The generalized finite-element method has become particularly popular in the computational modelling of propagating discontinuities such as cracks in solid materials. As shown by Belytschko *et al.* [5–9], crack discontinuities can be represented independently of the mesh by

*Correspondence to: E. A. Munts, Faculty of Aerospace Engineering, Delft University of Technology, P.O. Box 5058, 02600 GB Delft, The Netherlands.
†E-mail: e.a.munts@lr.tudelft.nl

Received 26 November 2002
Revised 4 May 2003

incorporating discontinuous fields into the standard displacement-based finite-element approximation using a partition-of-unity method. This formulation has the advantage of eliminating the need for pre-defined crack paths and remeshing procedures. Laghrouche *et al.* [10] employed the partition-of-unity concept for solving wave problems such as the diffraction of plane waves by cylinders and spheres. By incorporating harmonic enrichment functions into the approximation, wavelengths shorter than the element size could be represented accurately. As shown by Taylor *et al.* [11] and Duarte *et al.* [12], an alternative form of *p*-adaptivity can also be established by incorporating higher-order polynomial enrichment functions into the finite-element approximation. This concept was successfully applied in Reference [13] to overcome volumetric locking during plastic flow.

In many fluid-dynamic applications it would be beneficial to represent strong continuous variations in the solution using relatively coarse meshes, for example, in viscous regions associated with wall-bounded flows. In this paper, we consider the performance of the partition-of-unity method on a model problem for such phenomena, the solution of the linear diffusion equation for Stokes' second problem. We consider two types of enrichment functions, one containing characteristics of the analytic solution, and one corresponding to the higher-order approximation described in Reference [11].

We show that the choice of an enrichment function appropriate for diffusion-dominated regions can have implications for the computation of convective phenomena. In general, Galerkin finite-element discretizations require additional stabilization operators in order to compute convection-dominated problems. Recently, such stabilization operators have been reinterpreted in a multiscale framework [14, 15]. We illustrate that the partition-of-unity method can also be interpreted as a multiscale method, and that the choice of enrichment effects the convective stabilization properties of the scheme. We illustrate this effect using results obtained from a dispersion analysis for the linear convection case.

2. MODEL PROBLEM AND SPACE–TIME DISCRETIZATION

We consider the linear convection–diffusion equation in an open domain $\Omega =]0, 1[$, with appropriate boundary and initial conditions

$$\begin{aligned} u_{,t} + \lambda u_{,x} - \nu u_{,xx} &= 0 \quad \text{in } \Omega \\ u(x,0) &= u_0(x) \\ u(0,t) &= g_0(t) \\ u(1,t) &= g_1(t) \end{aligned} \tag{1}$$

where $\nu \geqslant 0$ is the constant diffusion coefficient and λ the constant convection speed.

The basis of our formulation is the so-called *time-discontinuous Galerkin method*. The Galerkin method, and the similarly the time-discontinuous Galerkin method lack stability in the sense that spurious oscillations are produced in the presence of unresolved internal and boundary layers. To improve upon this stability, while maintaining the order of accuracy, a least-squares operator is typically added to the Galerkin formulation.

Consider a space–time domain, where the time interval $]0, T[$ is subdivided into N intervals $I_n =]t_n,\ t_{n+1}[,\ n = 0, 1, \ldots, N-1$. Then, for each time interval we define a 'space–time slab'

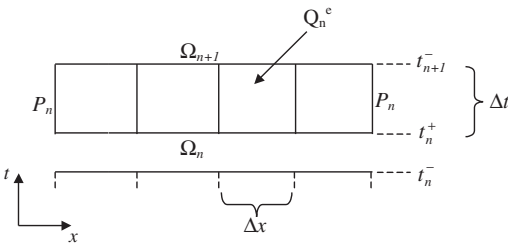

Figure 1. Example of a two-dimensional space–time slab Q_n with quadrilateral space–time elements Q_n^e.

$Q_n = \Omega \times I_n$ and its boundary $P_n = \Gamma \times I_n$, where Γ represents the boundary of the spatial domain Ω, see Figure 1. Finally, the slabs are decomposed into space–time elements Q_n^e, $e = 1, 2, \ldots, (n_{el})_n$.

Given a trial solution space V and a weighting space W the finite-element variational statement for (1) becomes: *Within each* Q_n, $n = 0, 1, \ldots, N-1$, *find* $u \in V$ *such that* $\forall w \in W$

$$\int_{Q_n} (-w_{,t}u - \lambda w_{,x}u + \nu w_{,x}u_{,x})\,\mathrm{d}Q + \int_{\Omega} (w(t_{n+1}^-)u(t_{n+1}^-) - w(t_n^+)u(t_n^-))\,\mathrm{d}\Omega$$

$$+ \sum_{e=1}^{(n_{el})_n} \int_{Q_n} L(w)\tau L(u)\,\mathrm{d}Q + \int_{P_n} (w(\lambda u - \nu u_{,x})n_x)\,\mathrm{d}P = 0 \tag{2}$$

The first two and last integrals constitute the time-discontinuous Galerkin method. The time-boundary integral resulting from applying the divergence theorem in space–time is added to the *jump term*

$$\int_{\Omega} w(t_n^+)(u(t_n^+) - u(t_n^-))\,\mathrm{d}\Omega \tag{3}$$

to give the second integral in (2). This jump-term provides the mechanism for advancing the solution from one slab to the next, by imposing a weakly enforced initial condition on the space–time slabs.

The third integral is the *least-squares operator* [16], which is defined only in the element's interior, where L is the convection–diffusion differential operator defined by

$$L = \frac{\partial}{\partial t} + \lambda \frac{\partial}{\partial x} - \nu \frac{\partial^2}{\partial x^2} \tag{4}$$

and τ is a scalar parameter of dimension time defined according to [17] as

$$\tau = \left(\left(\frac{2}{\Delta t} \right)^2 + \left(\frac{2\lambda}{\Delta x} \right)^2 + 9 \left(\frac{4\nu}{\Delta x^2} \right)^2 \right)^{-1/2} \tag{5}$$

where Δt is the time step and Δx is the mesh width in the space-direction of the elements. Note that the least-squares operator is not added for all computations.

To evaluate the integrals standard Gaussian quadrature is used, where for each computation a sufficient number of integration points is employed to ensure independence from quadrature error.

3. THE PARTITION-OF-UNITY METHOD

In the partition-of-unity method (PUM) enrichment functions are incorporated into the standard finite-element approximation as follows:

$$u^h(x,t) = \sum_{i=1}^{(n_n)_n} \varphi_i(x,t) \left(a_i + \sum_{j=1}^{n_e} \gamma_j(x,t) b_{ij} \right) \tag{6}$$

Here, $\varphi_i(x,t)$ is the finite-element shape function (constituting a partition of unity), a_i is the discrete value associated with node i, $(n_n)_n$ is the total number of nodes of the nth slab, γ_j contains n_e enrichment functions and b_{ij} are the discrete values associated with node i.

The nodal values a_i can be considered to be the standard finite-element nodal degrees of freedom, while the nodal values b_{ij} are additional degrees of freedom, one for each enrichment function. An essential feature is the multiplication of the enrichment functions by the nodal shape functions. This ensures the support of the enrichment and the shape function to be identical, and makes it straightforward to implement in existing finite-element codes. Moreover, the enrichment is able to take on a local form by enriching only those nodes whose support intersects regions of interest.

In general, the enrichment functions cannot be chosen arbitrarily. In order to form a basis for the approximation space, the finite-element shape functions and the enrichment functions must be *linearly independent*. In this paper, we will only consider (*bi*)*linear* finite-element shape functions for $\varphi_i(x,t)$ as the basis of our formulation, and therefore, enrichment with constant or linear functions, as well as pairs of functions of γ_j that are linearly dependent, are excluded.

3.1. The partition-of-unity method as a multiscale method

The partition-of-unity method can be interpreted in the framework of the 'variational multiscale method', as introduced by Hughes [15]. In the variational multiscale method, both the solution and the weighting functions are decomposed *a priori* into so-called *coarse* and *fine-scale* components defined by

$$u = \bar{u} + u' \tag{7}$$

$$w = \bar{w} + w' \tag{8}$$

where $\bar{u}$ corresponds to the *coarse-scale solution* and u' to the *fine-scale solution*. Similarly, $\bar{w}$ and w' correspond to the coarse-scale and fine-scale weighting function, respectively. When a mesh-based method is used, such as the finite-element method, the coarse and fine-scale components of the solution can be regarded as the *resolved field* and the *subgrid scales*. Substitution of these coarse and fine-scale components into the problem's variational statement

and requiring the coarse and fine-scale weighting functions to be linearly independent then leads to a set of two variational equations, the so-called coarse and fine-scale equations.

Considering the approximate solution of the partition-of-unity method, Equation (6), the following observation can be made. Since we use (bi)linear finite-element shape functions only, approximation (6) can be decomposed into a (bi)linear component (u_l) and an enriched component (u_e), given by

$$u_l = \sum_{i=1}^{(n_n)_n} \varphi_i a_i \tag{9}$$

$$u_e = \sum_{i=1}^{(n_n)_n} \sum_{j=1}^{n_e} \varphi_i \gamma_j b_{ij} \tag{10}$$

By choosing a Galerkin discretization for both the linear and enriched components of the solution, an additional set of variational equations is obtained for the unknowns b_{ij}, similar to the fine-scale equation of the variational multiscale method. We can therefore interpret the partition-of-unity method as a multiscale method, in which the resolved field corresponds to the linear component of the solution and subgrid-scale phenomena can be modelled by choosing an appropriate enrichment space.

As pointed out by Hughes [14], *stabilization operators* can also be interpreted as subgrid-scale models. In particular stabilization models using '*bubble-functions*' [18–20] or stabilization methods of *adjoint type* can be derived by defining local Dirichlet problems [14] for the fine scales within an element, then substituting the fine-scale solution back into the coarse-scale equation. Although this approach cannot be followed for all enrichment functions, this interpretation implies that the choice of enrichment, and therefore the related subgrid-scale model, can affect the stabilization properties of the scheme. This is demonstrated in Section 5 for the partition-of-unity method by investigating the effect of a particular enrichment on the dispersion properties of the scheme.

3.2. *p-Adaptivity by polynomial enrichment*

In principle, any function can be chosen as enrichment function, as long as the conditions mentioned in Section 3 are satisfied. By choosing polynomial enrichment functions, as shown by Taylor *et al.* [11], the partition-of-unity method can be used as an alternative form of *p*-adaptivity. In order to construct a quadratic approximation basis in space–time using three-node triangular space–time elements with standard linear shape functions, the following enriched basis can be employed

$$\gamma_j = \{(t-t_i)^2, (t-t_i)(x-x_i), (x-x_i)^2\} \tag{11}$$

where t_i and x_i are the co-ordinates of the nodes being enriched. Substituting this form into (6), the total approximation on a triangular element can be written in matrix notation as

$$u(x,t) = \sum_{i=1}^{3} \varphi_i(x,t) \left(a_i + \begin{bmatrix} (t-t_i)^2 & (t-t_i)(x-x_i) & (x-x_i)^2 \end{bmatrix} \begin{bmatrix} b_{i1} \\ b_{i2} \\ b_{i3} \end{bmatrix} \right) \tag{12}$$

Note that this approximation consists of four degrees of freedom per node, one corresponding to the standard finite-element approximation, a_i, and three enriched degrees of freedom corresponding to the enrichment functions, b_{i1}, b_{i2} and b_{i3}. The key difference with standard high-order methods is that the extra degrees of freedom are now located at existing nodes rather than along the edges or within the element. It should be noticed here that this enriched basis can be readily extended to multiple space-dimensions by including similar terms for the other spatial directions, for example

$$\gamma_j = \{(t-t_i)^2,\ (t-t_i)(x-x_i),\ (x-x_i)^2,\ (t-t_i)(y-y_i),\ (x-x_i)(y-y_i),\ (y-y_i)^2\} \quad (13)$$

is the equivalent of enriched basis (11), but now for two space-dimensions. However, in this paper we do not consider more than one spatial dimension.

In order to have a full quadratic (third-order accurate) representation of the solution on the complete domain including the boundaries, the boundary conditions must also be specified with third-order accuracy. Note that the values of the enrichment functions are zero at the nodes, see (11). Therefore the value of a_i at a Dirichlet-boundary must be equal to the exact solution at the node location. The values of b_{i2} and b_{i3} do not contribute to the representation at the boundary, and are therefore to be determined as part of the solution. The value of b_{i1}, however, must be specified as a time-varying boundary condition. This can be done by solving the following variational statement:

$$\int_{P_n} w(u-g)\,\mathrm{d}P = \int_{P_n} (w_l + w_e)(u_l + u_e - g)\,\mathrm{d}P = 0 \quad (14)$$

along the P-boundaries for every space–time slab, where g represents the boundary condition along these boundaries, and for this case only $\gamma_1(t)$ is taken into account for the enriched part. Eliminating the known values for the linear part of (14), which are the values of g in the boundary nodes, results in two equations for the unknowns, b_{i1}, at the two time levels of the slab (see Figure 1). These values are then used as Dirichlet conditions for the discrete system.

4. RESULTS

In this section, we discuss the results obtained from the partition-of-unity method incorporating different enrichment functions. First we consider the linear diffusion equation and investigate the approximation error and efficiency of the method. Subsequently, we study the effects of the chosen enrichments on the solution of the linear convection equation.

4.1. The linear diffusion equation

We consider *Stokes second problem*, describing the shear flow above an infinite oscillating plate. This problem is described by the linear diffusion equation, which is obtained from (1) by setting λ to zero, and the following boundary conditions:

$$\begin{aligned} u_{,t} - \nu u_{,xx} &= 0 \quad \text{for } 0 < x < \infty \\ u(0,t) &= U_0 \cos(\omega t) \\ u(\infty,t) &= 0 \end{aligned} \quad (15)$$

where U_0 is the amplitude and ω is the frequency of the oscillating plate. The analytic solution of this problem is known and given by

$$u(x,t) = U_0 e^{-\eta x} \cos(\omega t - \eta x) \tag{16}$$

or, equivalently

$$u(x,t) = U_0 e^{-\eta x}(\cos(\eta x)\cos(\omega t)) + U_0 e^{-\eta x}(\sin(\eta x)\sin(\omega t)) \tag{17}$$

where the constant $\eta = \sqrt{\omega/2v}$. In order to solve this problem numerically on $0 \leqslant x \leqslant 1$, the boundary condition at infinity is replaced by one at $x = 1$ using the analytic value

$$u(1,t) = U_0 e^{-\eta} \cos(\omega t - \eta) \tag{18}$$

In the following, U_0 and ω are set to unity and $\eta = 5.0$ for all computations.

4.1.1. Enrichment based on the analytic solution. For problems more general than those considered here, the analytical solution is usually not available. It is therefore useful to consider the performance of the partition-of-unity method incorporating enrichment functions which only partially represent the behaviour of the analytic solution. Inspecting the analytic solution of the linear diffusion equation (17), we choose the following enrichment function:

$$\gamma(x) = e^{-(x-x_i)k\eta} - 1 \tag{19}$$

where x_i is the node which is being enriched, k is some arbitrary constant and the '-1' is added so that the solution at the nodes is equal to a_i, see (6). Notice that this enrichment function only includes the exponential spatial variation of the analytic solution, not the complete analytic spatial variation, which would also necessitate the use of the time-varying sine terms. Moreover, notice that only for $k = 1.0$ the exact exponential spatial variation of the analytic solution is obtained.

In Figure 2 the enriched solution for $k = 1.0$ at time $t = 2\pi$ is compared to the non-enriched solution, both obtained without incorporating the least-squares operator. For simplicity all the nodes in the computational domain have been enriched. The results were computed using quadrilateral elements with mesh spacing $\Delta x = 0.25$ and $\Delta t = \pi/10$. The enriched approximation is in excellent agreement with the exact solution using only four elements per space–time slab. Notice that in the element's interior the enriched solution also closely follows the exact solution, in contrast to the standard piecewise-linear approximation.

4.1.2. Polynomial enrichment. Figure 3 shows the results for the diffusion problem using polynomial enrichment. The results were computed are shown for $t = 2\pi$ using triangular elements with $\Delta x = 0.25$ and $\Delta t = \pi/10$. It is seen that the polynomial-enriched solution is in better agreement with the analytic solution than the linear finite-element solution. At this level of discretization, however, it is not as accurate as the exponential-enriched solution. The relative accuracy of the exponential and polynomial enrichments is considered in more detail in the next section.

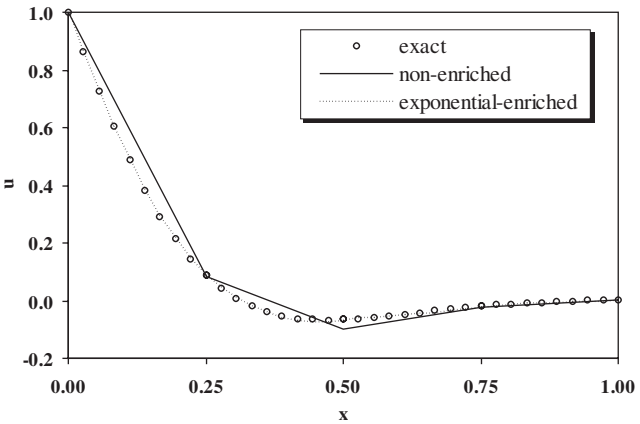

Figure 2. Exact, linear finite-element and exponential-enriched solution (with $k = 1.0$) of the linear diffusion equation at $t = 2\pi$ and $\eta = 5.0$ using four quadrilateral elements ($\Delta x = 0.25$ and $\Delta t = \pi/10$).

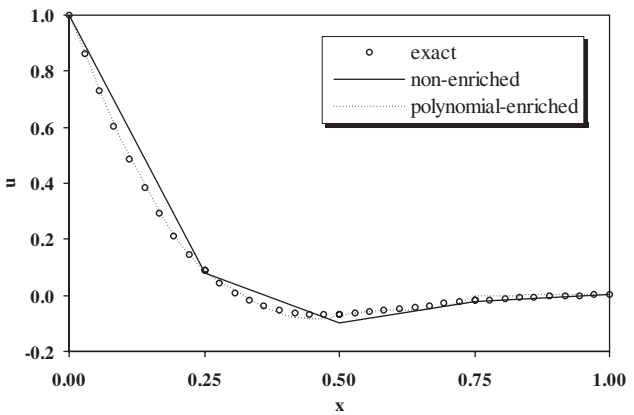

Figure 3. Exact, linear finite-element and polynomial-enriched solution of the linear diffusion equation at $t = 2\pi$ and $\eta = 5.0$ using four triangular elements ($\Delta x = 0.25$ and $\Delta t = \pi/10$).

4.1.3. Approximation error and efficiency. In order to compare the solution convergence behaviour, we consider the discrete L_2-norm of the error, computed according to

$$\|u - u^h\|_{L_2} = \left(\frac{1}{n} \sum_i \sum_j (u(x_i, t_j) - u^h(x_i, t_j))^2 \right)^{-1/2} \tag{20}$$

The results obtained for the diffusion equation by refining the mesh simultaneously in space and time are shown in Figure 4. It is seen from the slopes of the curves that the partition-of-unity method with exponential enrichment (19) has a slightly higher convergence rate than the linear finite-element method, which is of second order. As expected, the partition-of-unity method with polynomial enrichment (11) shows third-order convergence behaviour.

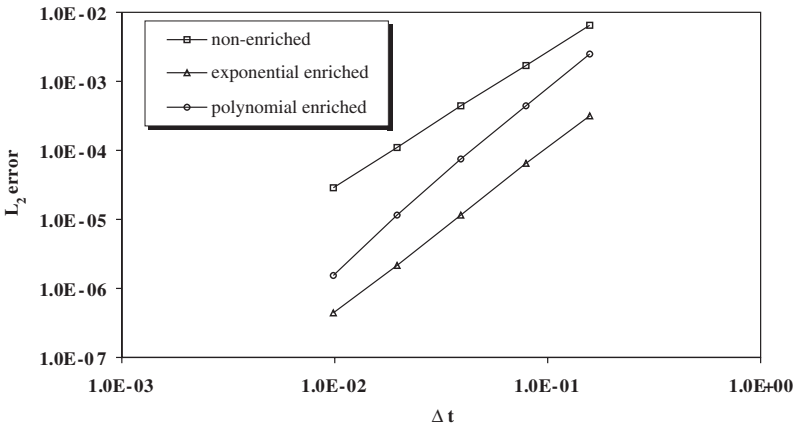

Figure 4. Convergence rates for the linear finite-element method and the partition-of-unity method with exponential and polynomial enrichment.

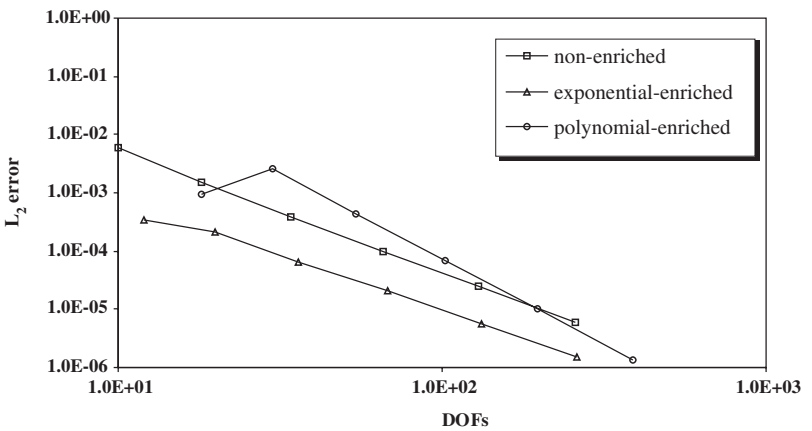

Figure 5. Efficiency of the partition-of-unity method using exponential and polynomial enrichment compared to the standard finite-element method.

Furthermore, it can be seen from Figure 4 that the partition-of-unity method with exponential enrichment is clearly the most accurate for coarse meshes. For finer meshes, there will be a cross-over point for which the polynomial-enriched approximation becomes more accurate because of its higher convergence rate.

The partition-of-unity method requires additional degrees of freedom compared to the standard finite-element method, depending on the number enrichment functions and the number of enriched nodes. It is therefore interesting to compare the efficiency of the methods by considering the error obtained for a given number of degrees of freedom (Figure 5). For the range of degrees of freedom investigated, the partition-of-unity method with exponential enrichment turns out to be the most efficient. Again, because of its higher convergence rate, there

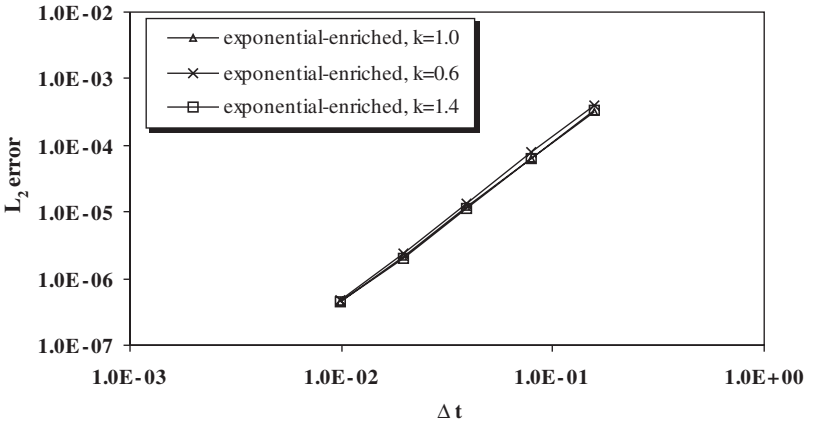

Figure 6. Accuracy of the partition-of-unity method with exponential enrichment for varying values of k.

will be a cross-over point after which the polynomial enriched approximation becomes more efficient. Note that in order to carry out the numerical integration to obtain the coefficients of stiffness matrix of the problem, more integration points are needed for the partition-of-unity method compared to the standard finite-element method. However, the corresponding increase in runtime is considerably less than the increase in runtime associated with solving a larger system.

It should be reiterated that the exponential enrichment considered in Figure 5 only partly represents the spatial variation of the analytic solution. The results in Figure 5 therefore confirm the benefits of introducing approximate solutions into the finite-element approximation space. The robustness of this technique can be demonstrated by considering values of k in (19) which deviate from unity. Figure 6 shows the accuracy obtained for $k = 0.6$, 1.0 and $k = 1.4$. It can be seen that the efficiency of the partition-of-unity method is retained for this wall-bounded flow even when a quite rough approximation of the analytic solution is employed.

4.2. *The linear convection equation*

As pointed out in Section 3.1, the choice of enrichment can be anticipated to affect the convective stabilization properties of the partition-of-unity method. We therefore investigate the effects of the enrichments discussed in the previous sections on the solution of the linear convection equation, obtained from (1) by setting v to zero, with an initial Gaussian wave and periodic boundary conditions, i.e.

$$\begin{aligned} u_{,t} + \lambda u_{,x} &= 0 \quad \text{for } 0 < x < 1 \\ u(x,0) &= \mathrm{e}^{-800(x-0.25)^2} \\ u(0,t) &= u(1,t) \end{aligned} \tag{21}$$

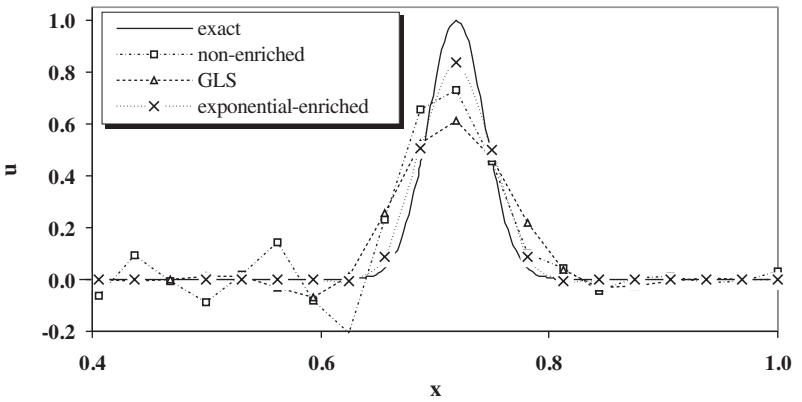

Figure 7. Convection of a Gaussian wave computed with the finite-element method, Galerkin/least-squares and the partition-of-unity method with exponential enrichment ($k = 1.0$) using quadrilateral elements and Courant number $C = 0.5$.

where the initial condition is set to zero if $u(x, 0) < 10^{-10}$. The analytic solution of the linear convection equation is then a simple translation of the initial wave, which, due to the periodic boundary condition, will re-enter the domain on the left as it exits on the right.

First, we consider the enrichment function based on the analytic solution of the linear diffusion equation, i.e. the exponential enrichment function (19). Since we are dealing with pure convection, there is no analytic constant for the exponent, so we assume

$$\gamma(x) = \mathrm{e}^{k_c(x-x_i)} - 1 \tag{22}$$

where k_c is now an arbitrary constant.

In Figure 7 the piecewise-linear solutions with and without the least-squares operator are compared with the exponential-enriched solution for $k = 1.0$, using quadrilateral elements and a *Courant number* $C = \lambda \Delta x / \Delta t = 0.5$. As discussed in Section 2, severe oscillatory behaviour is observed for the standard linear solution without least-squares operator. Including the least-squares operator eliminates the majority of the oscillations, but also leads to excessive decay of the initial wave. The exponential-enriched solution does remarkably well, showing no oscillations and a quite good representation of the peak, in contrast to the other two solutions.

Next, we consider the effect of the polynomial enrichment as presented in Section 3.2 on the linear convection problem. In Figure 8 the linear solutions with and without the least-squares operator are compared with the polynomial-enriched solution for $C = 0.5$, but now for triangular elements. The linear solution without least-squares operator is again oscillatory, although less than observed for quadrilateral elements. This is due to the fact that for the chosen orientation of the triangles the characteristics of the wave propagation are almost aligned with the element boundaries. As a consequence, the exact solution can be captured well using a standard space–time finite-element approximation [21]. The least-squares solution is not oscillatory, however excessive damping of the initial peak is again observed. The polynomial-enriched solution is also slightly oscillatory, comparable to the standard finite-element solution.

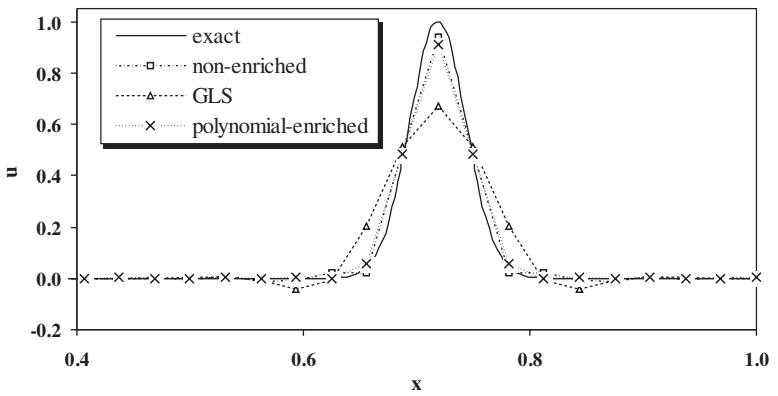

Figure 8. Convection of a Gaussian wave computed with the finite-element method, Galerkin/least-squares and the partition-of-unity method with polynomial enrichment using triangular elements and Courant number $C = 0.5$.

5. DISPERSION ANALYSIS

In this section we consider results from a dispersion analysis of the partition-of-unity method incorporating the enrichment functions discussed in the previous section for the linear convection equation. As discussed in Reference [21] amplification factors can be derived by assuming a solution of the form $e^{a(n\Delta t)}e^{i\beta}$ and solving for $\sigma = e^{a(n\Delta t)}$. Here $\beta = \kappa\Delta x$ is the spatial wave number which takes on M discrete values, where M is the number of elements which span the periodic domain. The amplitude and phase of a given discrete wave number can then be expressed relative to their exact counterparts as

$$\text{relative amplitude} = |\sigma_m| \tag{23}$$

$$\text{relative phase} = -\tan^{-1}\left(\frac{\text{Im}(\sigma_m)}{\text{Re}(\sigma_m)}\right)(C\beta)^{-1} \tag{24}$$

where C is the Courant number. The errors in amplitude and phase are thus given by the deviation from unity.

Figure 9 shows the computed relative phase and amplitude for the partition-of-unity method incorporating the exponential enrichment (22) with $k_c = 1.0$ and the Galerkin/least-squares method using quadrilateral elements. It is seen that for $C = 0.5$ the partition-of-unity method has very low phase and amplitude error, explaining the favourable result observed in Figure 7. In terms of the variational multiscale framework, one could thus say that for lower Courant numbers, the enrichment acts as a near-optimal subgrid-scale model. The Galerkin/least-squares solution exhibits considerably larger amplitude errors at this Courant number, since this method is specifically designed to damp high frequencies in order to prevent their high phase errors from polluting the solution. For larger Courant numbers, the phase and

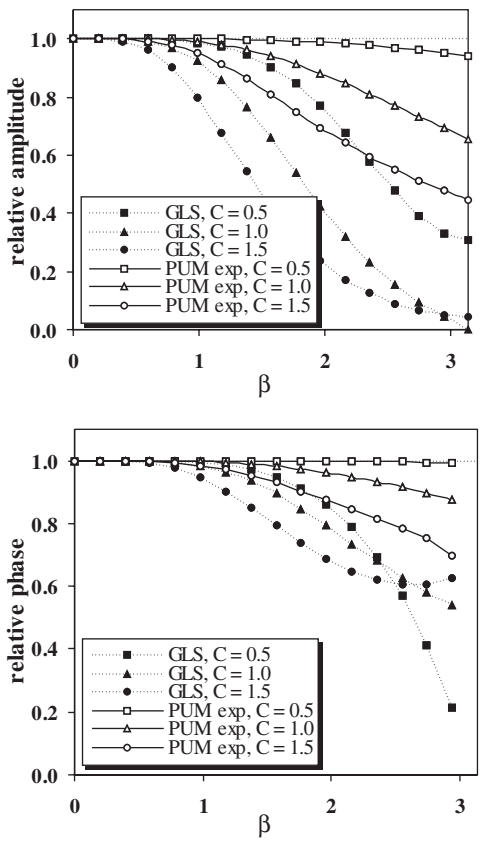

Figure 9. Relative amplitude and phase for the partition-of-unity method using exponential enrichment (with $k = 1.0$) and the Galerkin/least-squares method.

amplitude errors of the exponential-enriched solution increase, the latter providing convective stabilization by damping the inaccurate high-frequency modes.

In Figure 10 the relative amplitude and phase of the partition-of-unity method using polynomial enrichment are shown and compared to those obtained from the exponential enrichment and the Galerkin/least-squares method for a Courant number of 1.5. It is seen that the relative amplitude for the polynomial enrichment is superior to that of the exponential enrichment at this Courant number, however, large phase errors are observed for the high frequency modes. These are observed as oscillatory behaviour in the computed solution of Figure 5.

6. CONCLUSIONS

We have investigated the performance of the partition-of-unity method for convection–diffusion problems. First, we considered the linear diffusion problem, or Stokes' second problem, using exponential enrichment based on an approximation of the time-independent component of the

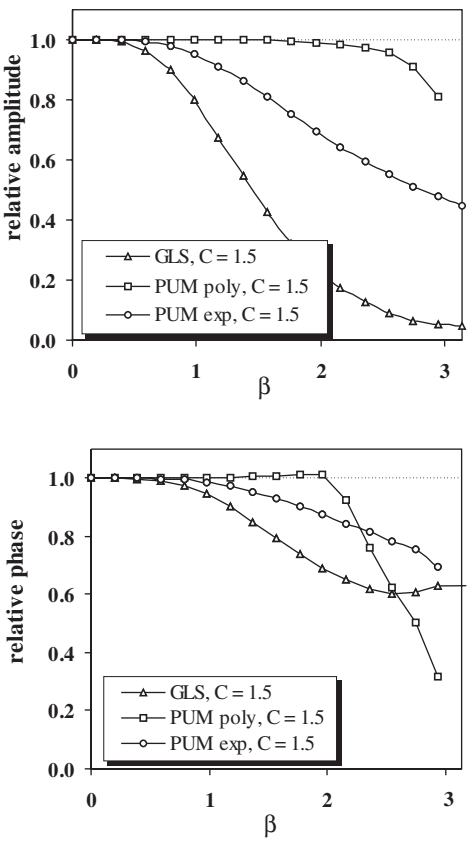

Figure 10. Relative amplitude and phase for the partition-of-unity method using polynomial and exponential enrichment (with $k = 1.0$) and the Galerkin/least-squares method for $C = 1.5$.

analytic solution. It was shown that this approach leads to an increase in accuracy for a given number of degrees of freedom, when compared with the standard finite-element method. This increased efficiency is retained even when rough approximations are used. We also considered the use of polynomial enrichment in the partition-of-unity method. It was shown that higher-order accuracy can be obtained using this approach, although its efficiency is generally lower than that of the exponential enrichment for the problems considered here.

We have investigated the implications of the choice of enrichment on the computation of convection phenomena. As the enriched basis can be interpreted as a fine-scale model of a multiscale approach, it can be anticipated that its chosen form can influence the stabilization properties of the method. It was shown that for low Courant numbers, the method using exponential enrichment has very low phase and amplitude errors and thus acts as a near optimal subgrid-scale model. The polynomial enrichment has low phase errors but large phase errors for the high-frequency modes. Its stability is less optimal than that of the exponential-enriched scheme.

REFERENCES

1. Strouboulis T, Babuška I, Copps K. The design and analysis of the Generalized Finite Element Method. *Computer Methods in Applied Mechanics and Engineering* 2000; **181**:43–69.
2. Babuška I, Melenk J. The Partition-of-unity Method. *International Journal for Numerical Methods in Engineering* 1997; **40**:727–758.
3. Melenk J, Babuška I. The partition-of-unity finite element method: Basic Theory and applications. *Computer Methods in Applied Mechanics and Engineering* 1996; **139**:289–314.
4. Strouboulis T, Copps K, Babuška I. The generalized finite element method: an example of its implementation and illustration of its performance. *International Journal for Numerical Methods in Engineering* 2000; **47**: 1401–1417.
5. Daux C, Moës N, Dolbow J, Sukumar N, Belytschko T. Arbitrary branched and intersecting cracks with the extended finite element method. *International Journal for Numerical Methods in Engineering* 2000; **48**: 1741–1760.
6. Dolbow J, Moës N, Belytschko T. An extended finite element method for modeling crack growth with frictional contact. *Computer Methods in Applied Mechanics and Engineering* 2001; **190**:6825–6846.
7. Moës N, Belytschko T. Extended finite element method for cohesive crack growth. *Engineering Fracture Mechanics* 2002; **69**:813–833.
8. Moës N, Dolbow J, Belytschko T. A finite element method for crack growth without remeshing. *International Journal for Numerical Methods in Engineering* 1999; **46**:131–150.
9. Sukumar N, Moës N, Moran B, Belytschko T. Extended finite element method for three-dimensional crack modelling. *International Journal for Numerical Methods in Engineering* 2000; **48**:1549–1570.
10. Laghrouche O, Bettess P, Astley RJ. Modelling of short wave diffraction problems using approximating systems of plane waves. *International Journal for Numerical Methods in Engineering* 2002; **54**:1501–1533.
11. Taylor RL, Zienkiewicz OC, Oñate E. A hierarchical finite element method based on the partition-of-unity. *Computer Methods in Applied Mechanics and Engineering* 1998; **152**:73–84.
12. Duarte CA, Babuška I, Oden JT. Generalized finite element methods for three dimensional structural mechanics problems. *Computers and Structures* 2000; **77**:215–232.
13. Wells GN, Sluys LJ, de Borst R. A p-adaptive scheme for overcoming volumetric locking during plastic flow. *Computer Methods in Applied Mechanics and Engineering* 2002; **191**:3153–3164.
14. Hughes TJR. Multiscale phenomena: Green's functions, the Dirichlet-to-Neumann formulation, subgrid scale models, bubbles and the origins of stabilized methods. *Computer Methods in Applied Mechanics and Engineering* 1995; **127**:387–401.
15. Hughes TJR, Feijóo GR, Mazzei L, Quincy J. The variational multiscale method—a paradigm for computational mechanics. *Computer Methods in Applied Mechanics and Engineering* 1998; **166**:3–24.
16. Hughes TJR, Franca LP, Hulbert GM. A new finite element formulation for computational fluid dynamics: VIII. The Galerkin/least-squares method for advective diffusive equations. *Computer Methods in Applied Mechanics and Engineering* 1989; **73**:173–189.
17. Shakib F, Hughes TJR. A new finite element formulation for computational fluid dynamics: IX. Fourier analysis of space–time Galerkin/least-squares algorithms. *Computer Methods in Applied Mechanics and Engineering* 1991; **87**:35–58.
18. Brezzi F, Russo A. Choosing bubbles for advection-diffusion problems. *Mathematical Models and Methods in Applied Sciences* 1994; **4**:571–587.
19. Baiocchi C, Brezzi F, Franca LP. Virtual bubbles and Galerkin/least-squares type methods (Ga.L.S.). *Computer Methods in Applied Mechanics and Engineering* 1993; **105**:125–141.
20. Brezzi F, Bristeau MO, Franca LP, Mallet M, Rogé G. A relationship between stabilized finite element methods and the Galerkin method with bubble functions. *Computer Methods in Applied Mechanics and Engineering* 1992; **96**:117–129.
21. Hulshoff SJ, Bijl H, de Borst R. Wave propagation in adaptive space–time computations. *WCCM V*, *Fifth World Congress on Computational Mechanics*, Vienna, Austria, 2002.

